Supporting Information

Chemodynamic/photothermal synergistic therapy based on Ce-doped Cu-Al layered double hydroxide

Zhengdi Wang,‡ Liyang Fu,‡ Yu Zhu, Sa Wang, Guohong Shen, Lan Jin*, Ruizheng Liang*

State Key Laboratory of Chemical Resource Engineering, Beijing Advanced Innovation Center for Soft Matter Science and Engineering, Beijing University of Chemical Technology, Beijing 100029, P. R. China.

E-mail addresses: liangrz@mail.buct.edu.cn (R. Liang); jinlan@mail.buct.edu.cn (L. Jin)
‡ These authors contributed equally to this work.

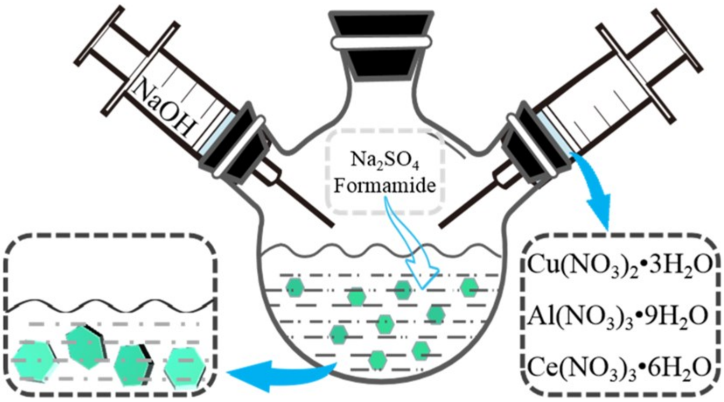

Scheme S1. Schematic illustration of the bottom-up method of synthesizing CuAlCe-LDH.

Table S1. The feed ratio and the actual ratio of LDH determined by ICP.

Sample	Feed ratio	Actual ratio	References
Cu Al-LDH	2 : 1	2.47 : 1	this work
Cu Al Ce-LDH	2 : 0.5 : 0.5	2.32 : 0.57 : 0.43	this work
Cu Al Ce-LDH	2 : 0.67 : 0.33	2.21 : 0.65 : 0.34	this work
Cu Al Ce-LDH	2 : 0.75 : 0.25	2.37 : 0.75 : 0.28	this work
Mg Al Ce-LDH	3 : 0.8 : 0.2	0.73 : 0.24 : 0.014	1, 2
Ni Fe Ce-LDH		doping 5% Ce	3

Table S2. The K_M and V_{max} values of different Fenton catalysts.

Sample	K_M (mM)	V_{max} ($M \cdot s^{-1}$)	References
ICG/CuAlCe-LDH	1.57	4.88×10^{-6}	this work
FeAl-LDH	0.16	1.47×10^{-6}	4
PEG/Fe-LDHs	0.09	1.76×10^{-6}	4
Fe_3O_4 NPs	26.08	6.17×10^{-8}	5
Mn-NS	26.40	7.04×10^{-8}	6
Fe_3O_4@PPy@GOD NCs	4.94	1.13×10^{-8}	7

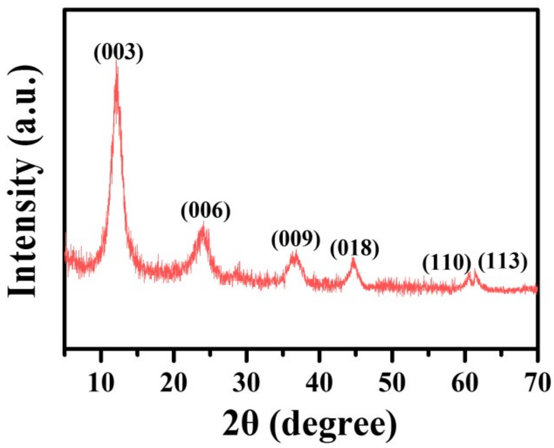

Fig. S1 XRD pattern of CuAl-LDH (2:1) nanosheets after restocking.

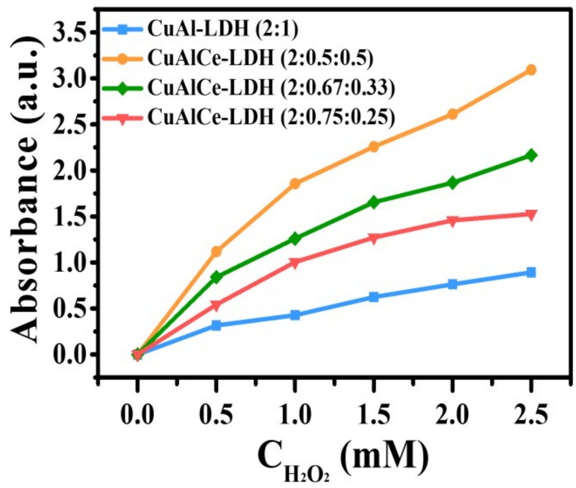

Fig. S2 H_2O_2 reacts with CuAl-LDH and CuAlCe-LDH to oxidate TMB at pH=6.5, and the absorbance (650 nm) of reactants is determined *via* UV spectrum.

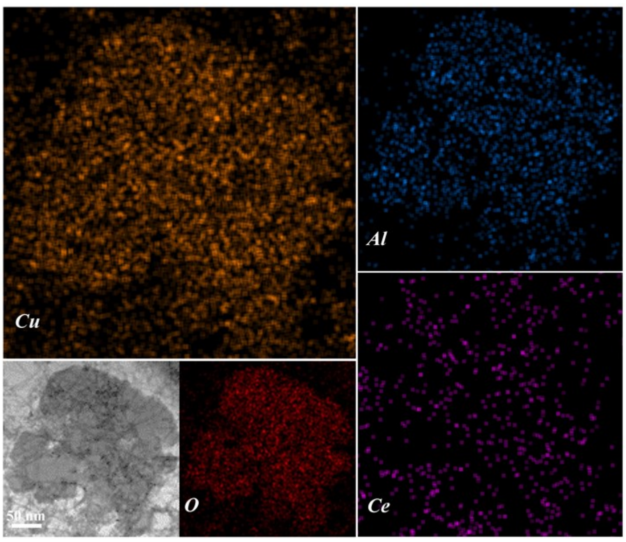

Fig. S3 TEM image of CAC-LDH nanosheets with corresponding EDX mapping images for Cu, Al, Ce and O, respectively.

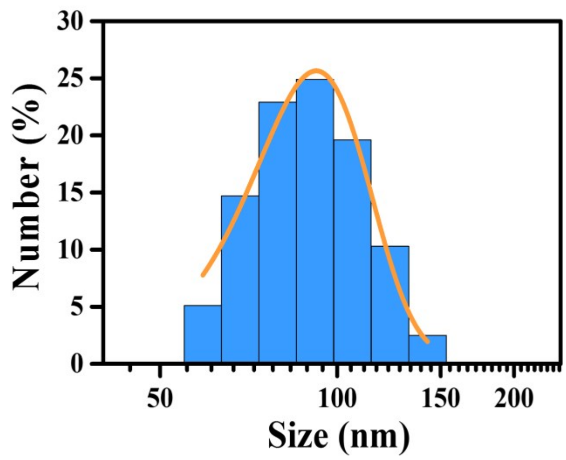

Fig. S4 The hydrodynamic size of CAC-LDH.

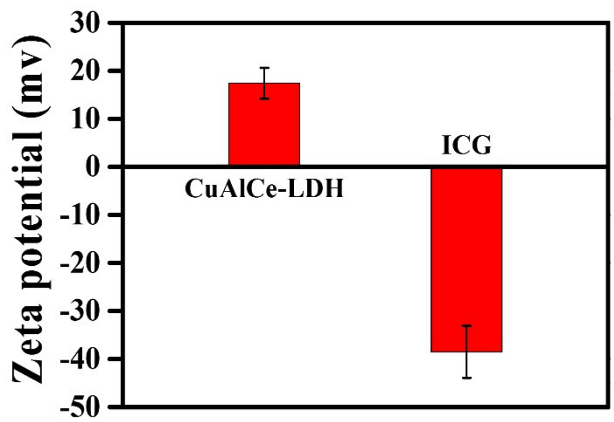

Fig. S5 Zeta potential of ICG and CAC-LDH.

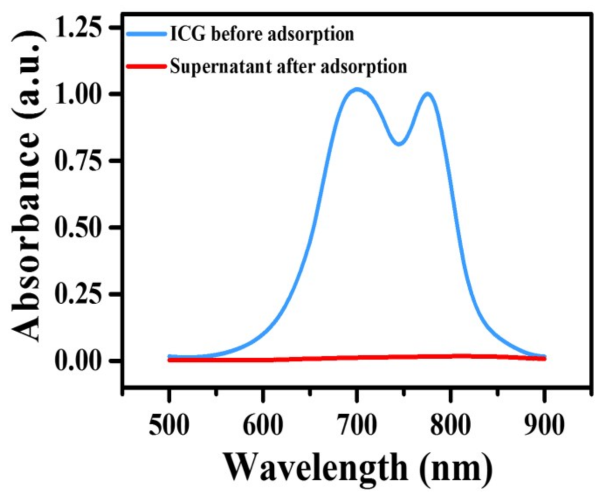

Fig. S6 The UV–vis–NIR of ICG aqueous solution before and after adsorption with CAC-LDH.

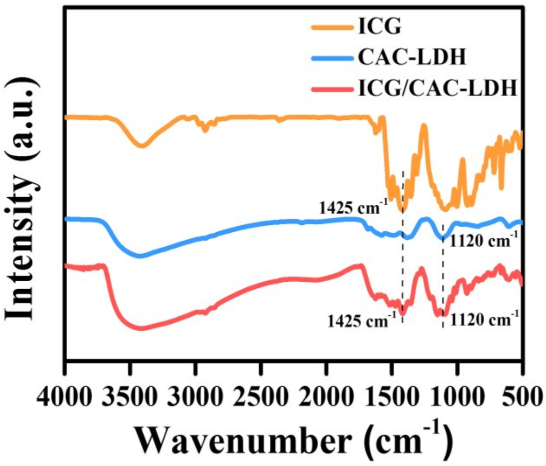

Fig. S7 FTIR spectra of CAC-LDH, ICG and ICG/CAC-LDH, respectively.

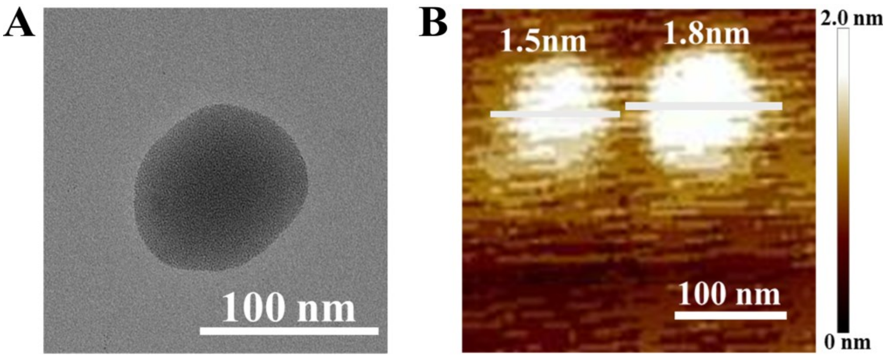

Fig. S8 (A) TEM and (B) AFM of ICG/CAC-LDH.

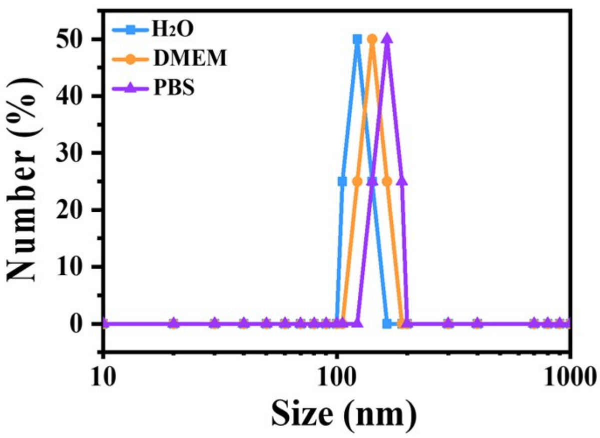

Fig. S9 Size distribution of ICG/CAC-LDH in water, PBS, and culture medium (DMEM).

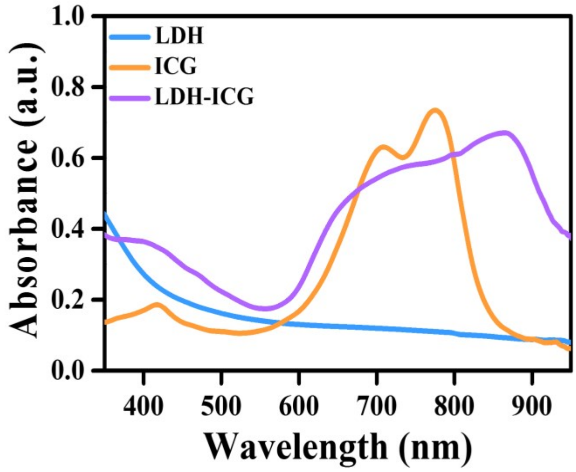

Fig. S10 UV–vis–NIR spectra of ICG, CAC-LDH and ICG/CAC-LDH, respectively.

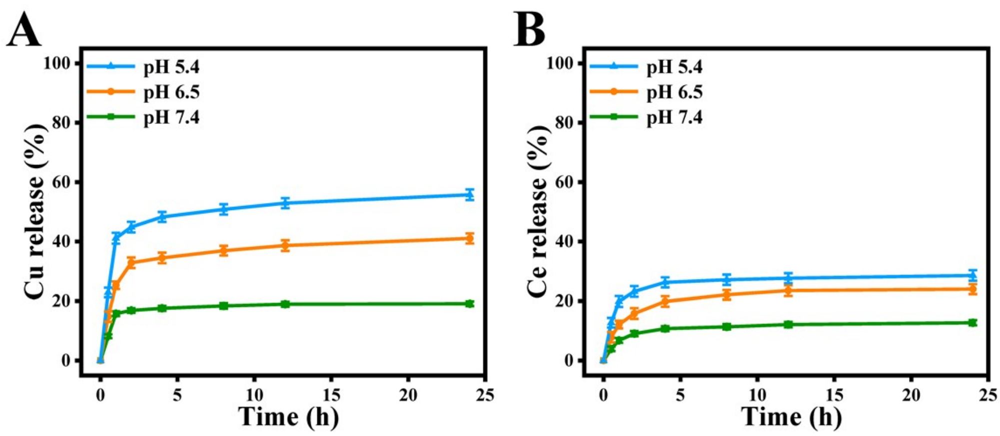

Fig. S11 Release profiles of copper (A) and cerium (B) from ICG/CAC-LDHs under various conditions. Error bars represented for standard deviation, n = 3.

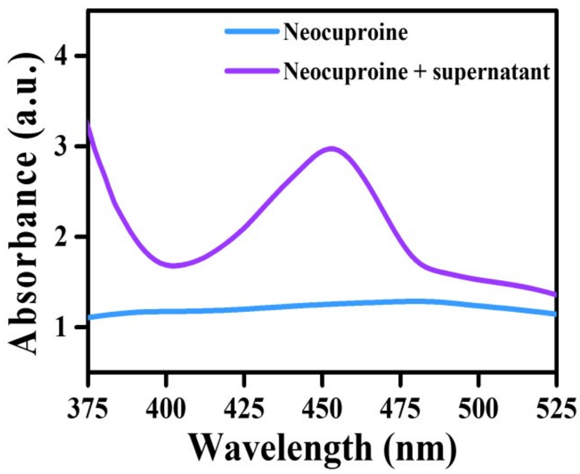

Fig. S12 Cu (I) detected by the selective sequestering agent neocuproine.

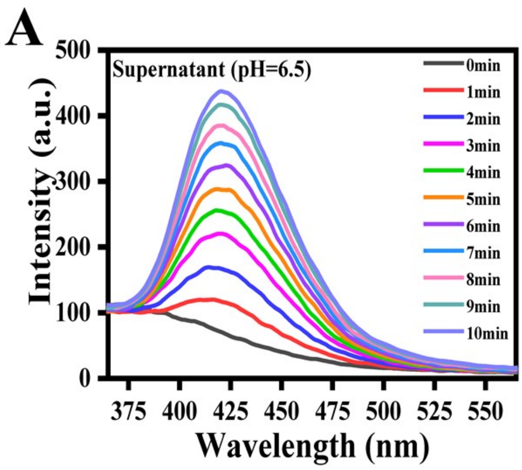

Fig. S13 FL spectra of terephthalate (TA) oxidized by ·OH generated from the reactions between ICG/CAC-LDH and H_2O_2: (A) without 808 nm laser irradiation; (B) with 808 nm laser irradiation.

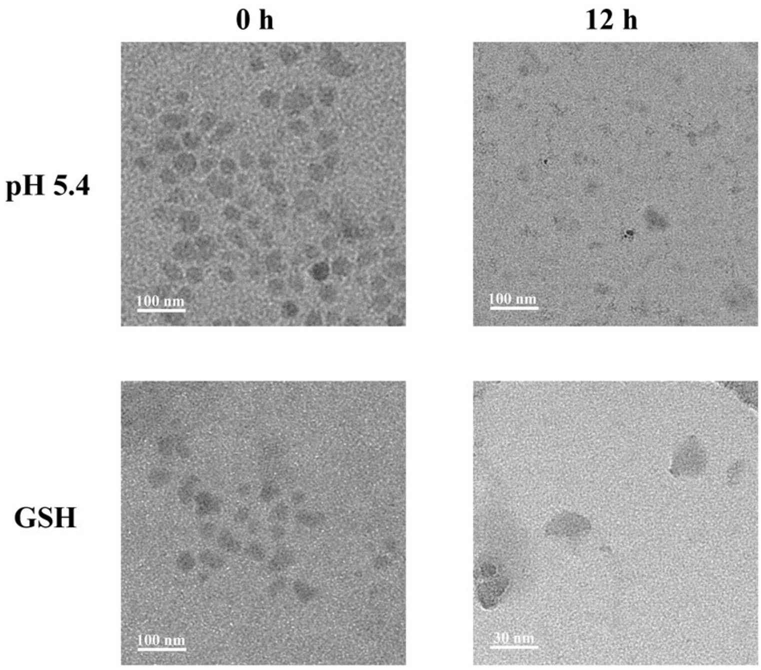

Fig. S14 TEM images of CAC-LDH after different treatments for various periods of time.

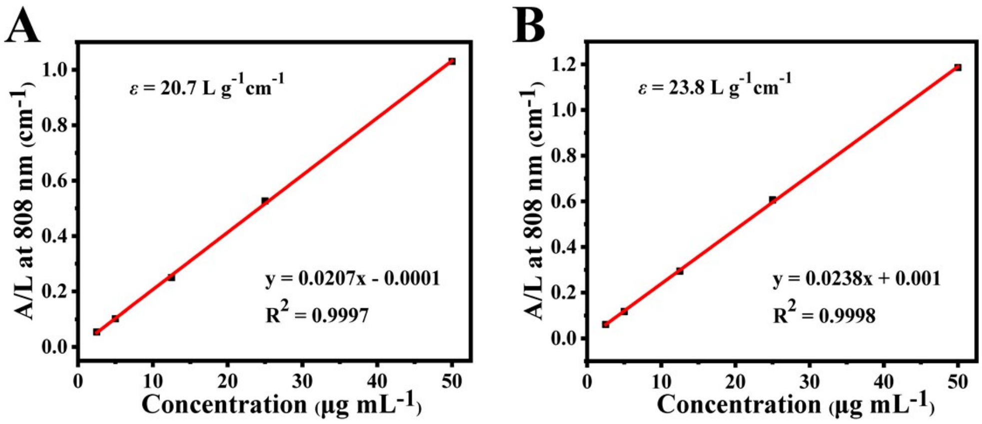

Fig. S15 Mass extinction coefficient of ICG (A) and ICG/CAC-LDH (B) at 808 nm. Normalized absorbance intensity at λ= 808 nm divided by the characteristic length of cell (A/L) at varying concentrations.

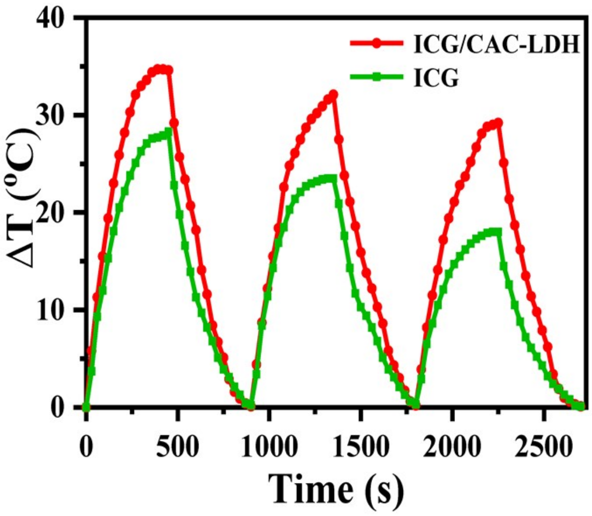

Fig. S16 Photostability tests of ICG and ICG/CAC-LDH for three cycles.

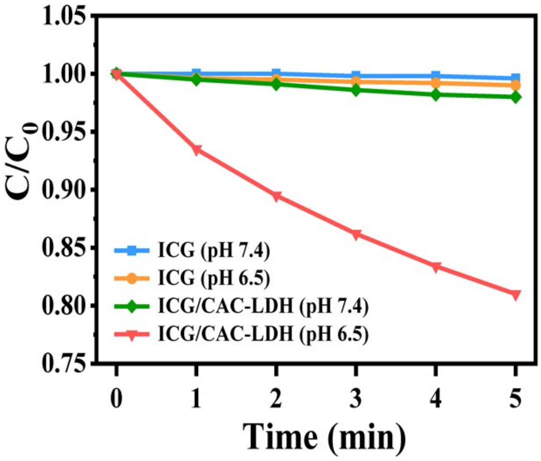

Fig. S17 Normalized absorbance of ICG and ICG/CAC-LDH at 808 nm in solutions at different pH values with H_2O_2 (0.1 mM).

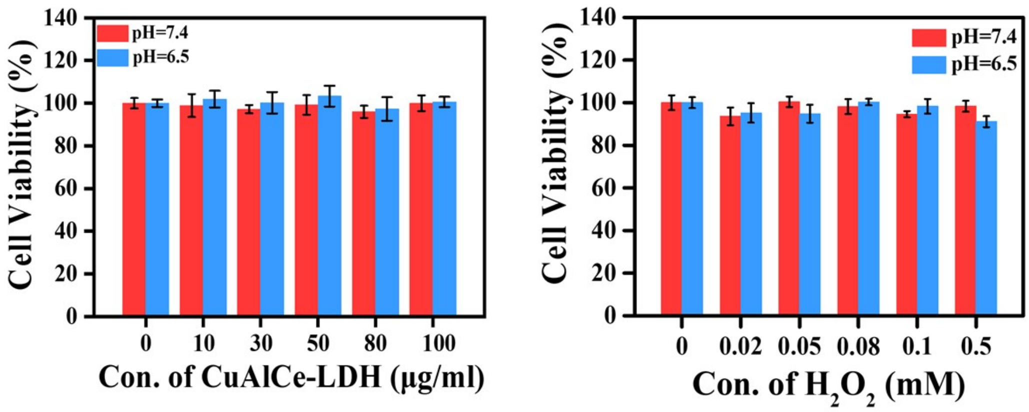

Fig. S18 Cytotoxicity tests with different concentrations of CuAlCe-LDH and H_2O_2 in different pH conditions.

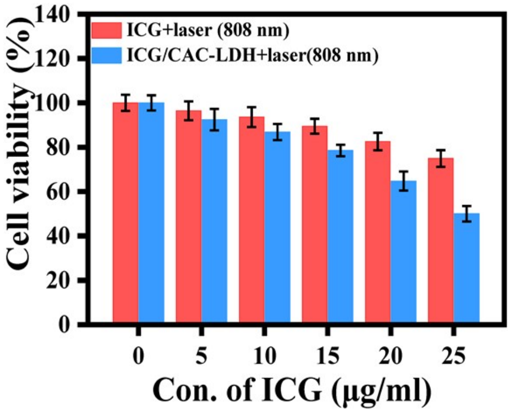

Fig. S19 Relative viabilities of HepG2 cells after incubated with ICG and ICG/CAC-LDH at various concentrations (quantified by ICG: 0, 5, 10, 15, 20, 25 μg·mL^{-1}) at pH 6.5 with 808 nm laser irradiation.

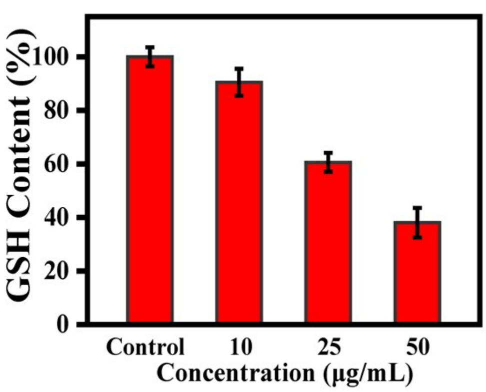

Fig. S20 GSH content of HepG2 cells treated with different concentrations of CAC-LDH (0−50 μg·mL^{-1}) for 24 h.

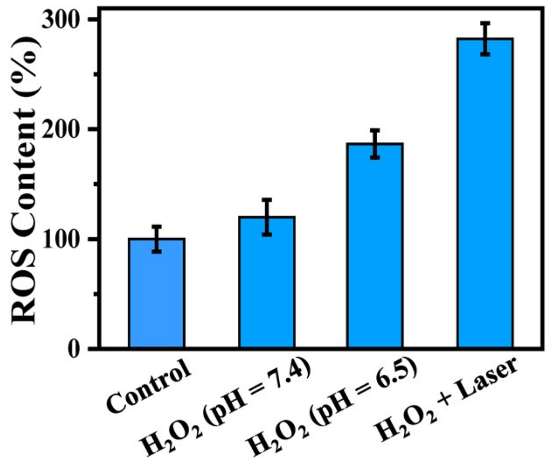

Fig. S21 ROS levels of DCFH-DA stained HepG2 cells with different treatments.

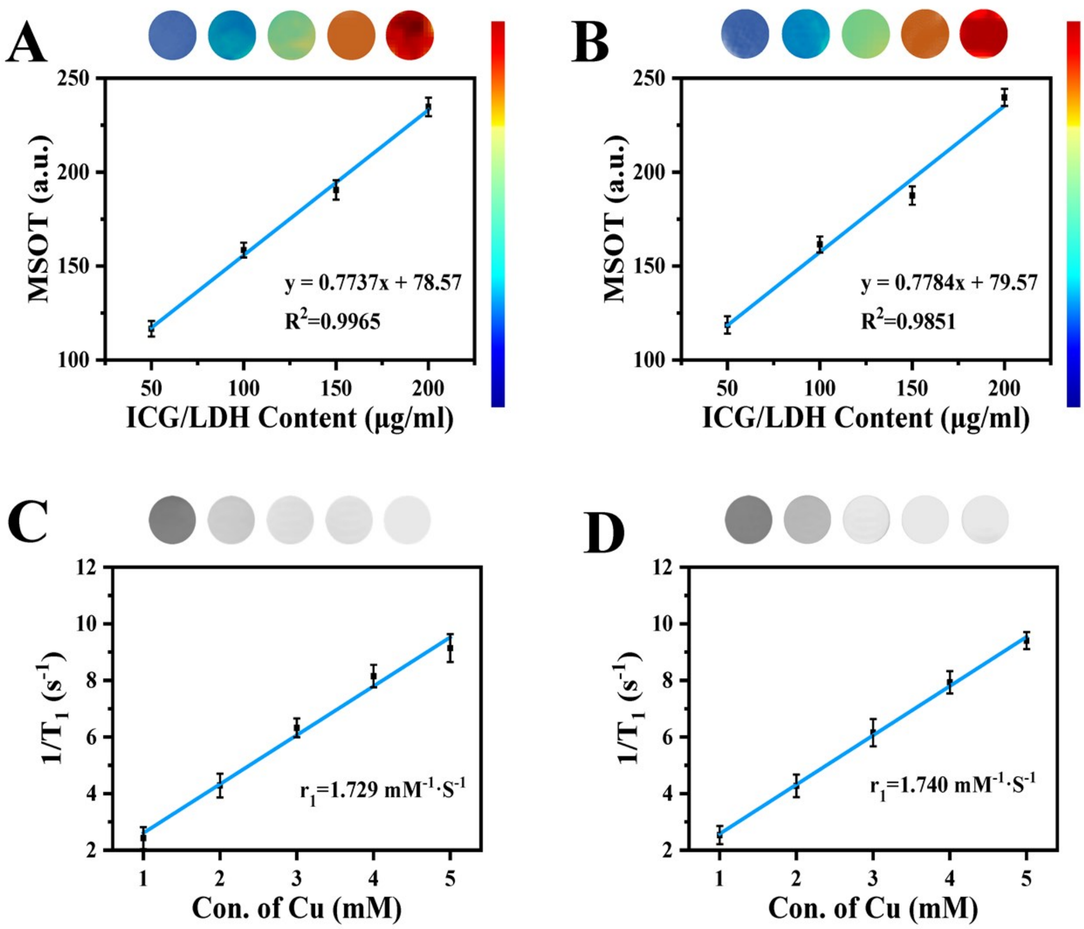

Fig. S22 Linear relationship between PA signal and ICG/CAC-LDH concentration under the conditions of (A) GSH (1 mM) and (B) H_2O_2 (0.1 mM). Linear relationship between T_1-MR signal and Cu(II) concentration under the conditions of (C) GSH (1 mM) and (D) H_2O_2 (0.1 mM).

REFERENCES

(1) K. W. Iqbal, A. Iqbal, A. M. Kirillov, B. K. Wang, W. S. Liu and Y. Tang, *J. Mater. Chem. A.*, 2017, **5**, 6716.
(2) K. W. Iqbal, A. Iqbal, A. M. Kirillov, C. F. Shan, W. S. Liu and Y. Tang, *J. Mater. Chem. A.*, 2018, **6**, 4515.
(3) H. J. Xu, B. K. Wang, C. F. Shan, P. X. Xi, W. S. Liu and Y. Tang, *ACS Appl. Mater. Inter.*, 2018, **10**, 6336−6345.
(4) Z. B. Cao, L. Zhang, K. Liang, S. S. Cheong, C. Boyer,J. J. Gooding, Y. Chen and Z. Gu, *Adv. Sci.*, 2018, **5**, 1801155.
(5) M. Huo, L. Wang, Y. Chen and J. Shi, *Nat. Commun*., 2017, **8**, 357.
(6) W. Tang, W. P. Fan, W. Z. Zhang, Z. Yang, L. Li, Z. T. Wang, Y. L. Chiang, Y. J. Liu, L. M. Deng, L. C. He, Z. Y. Shen, O. Jacobson, M. A. Aronova, A. Jin, J. Xie and X. Y. Chen, *Adv. Mater.*, 2019, **31**, 1900401.
(7) W. Feng, X. G. Han, R. Y. Wang, X. Gao, P. Hu, W. W. Yue, Y. Chen and J. L. Shi, *Adv. Mater.*, 2019, **31**, 1805919.